Juniper Online
Journal Material Science
ISSN: 2575-856X

Juniper PUBLISHERS key to the Researchers

Review Article
Volume 10 Issue 3 - March 2026
DOI: 10.19080/JOJMS.2026.10.555788

JOJ Material Sci

The Use of X-Ray Photoelectron Spectroscopy in Studying Azurite and Malachite as Minerals, Pigments and in Secondary Products on Copper Objects

J Theo Kloprogge*

Department of Chemistry, University of the Philippines Visayas, Philippines

Submitted: February 16, 2026; **Published:** March 18, 2026

***Corresponding author:** J Theo Kloprogge, Department of Chemistry, College of Arts and Sciences, University of the Philippines Visayas, Miagao, Iloilo 5023, Philippines

Abstract

This comprehensive analysis examines the oxidation state quantification and binding energy assignments in copper minerals, with particular emphasis on azurite [$Cu_3(CO_3)_2(OH)_2$] and malachite [$Cu_2CO_3(OH)_2$], using X-ray photoelectron spectroscopy (XPS). The primary objectives of this work are to: (1) establish precise binding energy values for distinguishing between copper oxidation states (Cu^+ and Cu^{2+}) and correlating these values with crystal structure variations; (2) document and interpret photo-induced reduction phenomena occurring during XPS measurement; (3) characterize how complex overlapping carbon and oxygen spectra reflect structural differences between mineralogically similar phases; (4) elucidate binding energy changes during corrosion, patina formation, and thermal degradation processes; and (5) develop practical quantification methodologies and best practices for analyzing aged pigments and archaeological copper-bearing artifacts. The work integrates empirical XPS data with theoretical understanding of how crystal field effects, local coordination geometry, and interfacial charge transfer modulate core-level binding energies. By providing detailed comparative analysis of azurite and malachite spectral features, including shake-up satellite structures, elemental atomic percentages, and deviations from theoretical stoichiometry, this study establishes a rigorous framework for XPS-based phase identification and compositional analysis of complex copper systems encountered in cultural heritage materials, corrosion studies, and heterogeneous catalysis applications.

Keywords: Azurite; Malachite; X-Ray Photoelectron spectroscy (XPS); Copper carbonate; Heritage conservation; Corrosion patterns; Pigments

Abbreviations: XPS: X-ray photoelectron spectroscopy; Cu2O: copper oxide; FTIR: Fourier Transform Infrared Spectroscopy; ATR: Attenuated Total Reflection; DRIFT: Diffuse Reflectance Infrared Fourier Transform; SORS: Spatially Offset Raman Spectroscopy; XRF: X-ray fluorescence spectroscopy; XRD: X-ray diffraction; EDS: Energy Dispersive X-ray Spectroscopy; SEM: scanning electron microscopy

Introduction

Azurite and malachite Figure 1 form from the supergene oxidation of primary copper sulfide assemblages (chalcopyrite, bornite, chalcocite) that precipitate in structurally controlled shear zones and fractures [1]. This has been responsible for some of the largest copper ore deposits in the world, where supergene enrichment has significantly enhanced copper grades in porphyry deposits, such as Bingham Canyon in the United States [2]. The vertical distribution of oxidation minerals is also a function of fluctuating groundwater levels and climatic cycles, where malachite and azurite define the upper parts of oxidation zones above primary sulfide assemblages [3]. In sedimentary copper deposits, copper mineralization is localized to areas of reduced siliciclastic facies where paleo-permeability features enhance sulfide precipitation [4]. The precipitation of secondary copper minerals is a function of oxidative dissolution of primary copper sulfide minerals that have been transported to an oxidizing environment above the water table, where their thermodynamic stability is controlled by pH and redox conditions [5]. The secondary copper minerals azurite ($Cu_3(CO_3)_2(OH)_2$) and malachite ($Cu_2CO_3(OH)_2$) precipitate under lower pH (4-6) and higher pH (7-9) conditions, respectively [5]. Malachite is a secondary copper mineral that is more thermodynamically

stable under Earth surface conditions and replaces azurite under prolonged weathering [6]. The formation of malachite is also enhanced by microbial-induced precipitation of carbonates, which facilitates copper immobilization from solution [7].

Figure 1: azurite from Malbunker Copper Mine, Western Aranda Country, Areonga, NT, Australia (left), slice of policed malachite from the Kason Pi Mine, Dem. Rep. Congo (right). Both in the author's collection under catalogue number C44 and C57.

The secondary copper mineral assemblages such as azurite, malachite, native copper, cuprite, and copper chlorides are the result of multi-stage supergene evolution processes [8]. The copper (II) oxide components of the azurite and malachite minerals are responsible for the characteristic blue and green colors of the minerals, respectively, by selective absorption of light of particular wavelengths [9,10]. Isotopic signatures of secondary carbonates indicate interaction with marine carbonates and meteoric waters, whereas the isotopic signatures of primary and secondary sulfides indicate mixed sources of ophiolitic and volcano-sedimentary rocks [1]. The isotopic signatures of the sediment-hosted deposits indicate diagenetic origins of the deposits from framboidal pyrite in the presence of reducing micro-environments that facilitate oxidation and secondary mineralization processes [4]. The geochemical and isotopic signatures indicate that the formation of azurite and malachite has occurred through multi-stage fluid-rock interaction processes under changing redox conditions [6].

The two most common types of basic copper carbonates are azurite, $Cu_3(CO_3)_2(OH)_2$, and malachite, $Cu_2CO_3(OH)_2$, both of which crystallize in the monoclinic system with the $P2_1/c$ space group, though they differ in the arrangement of the layers and the degree of hydration. Azurite contains three copper atoms per formula unit and has less water of crystallization than malachite, which contains two copper atoms per formula unit. The differences in the coordination environment of the copper atoms control the reactivity of the mineral and the color of the mineral, as well as the characteristic hydroxyl absorption bands in the infrared region of the spectrum. Malachite contains two different hydroxyl groups in the structure, resulting in the presence of two characteristic OH stretching absorption bands at 3314 and 3402 cm^{-1} in the infrared region of the spectrum [9-12]. Azurite contains only one type of hydroxyl group, resulting in only one characteristic OH stretching absorption band at 3424 cm^{-1} in the infrared region of the spectrum [9-12]. The differences in the structures of the two minerals are reflected in their thermal stability: malachite is stable up to 280°C due to the presence of hydrogen bonding between the hydroxide and carbonate groups, whereas azurite loses water at lower temperatures and begins to dehydrate at temperatures below 280°C [13]. Azurite has lower thermodynamic stability than malachite and can transform to malachite under moist conditions, explaining the association of the two minerals in the weathered zones of copper deposits [14]. The differences in the coordination environment of the copper atoms control the color of the mineral: whereas malachite has a green color, azurite has a deep blue color, and the differences in the structures of the two minerals control their reactivity in the supergene environment.

Both azurite and malachite have been prized by artists for at least two millennia, making them two of the most important and widely used artistic pigments. Azurite was the source of the characteristic blue pigment used in the illuminated manuscripts of the Middle Ages, where the pigment was used in the form of a finely ground powder mixed with a binder like egg yolks or animal glue [15]. The exceptional ability of the blue pigment derived from azurite, used in the illuminated manuscripts of the fifteenth and sixteenth centuries, can be attributed to the optical properties of the mineral and the advanced technology used in pigment processing during the Middle Ages [15] Figure 2a. Malachite, with its characteristic green color, provided the green pigment used in Russian icons and was used extensively in the Eastern Orthodox artistic traditions of the Middle Ages [16]. In addition to the use of the two copper carbonate hydroxide minerals in the artistic traditions of the Middle Ages, the use of the two minerals has been prominent in the polychrome paintings used in the architecture of the Ming dynasty, where the use of azurite for the blue and

How to cite this article:J Theo Kloprogge. The Use of X-Ray Photoelectron Spectroscopy in Studying Azurite and Malachite as Minerals, Pigments and in Secondary Products on Copper Objects. JOJ Material Sci. 2026; 10(3): 555788. DOI: 10.19080/JOJMS.2026.10.555788

malachite for the green pigment, has been identified in the early Ming dynasty polychrome paintings of Yuzhen Palace, along with vermilion and hematite for the red pigment, indicating the advanced technology used in the Ming dynasty pigment processing traditions [16]. Azurite and malachite were also used in the Byzantine iconography and other important artistic traditions of the past, spanning several centuries and several continents of the world Figure 2b, and are still used in the present day, as reported by [17].

Figure 2: (left) Illuminated manuscript leaf (15th century) showing the application of azurite (blue) and malachite (green) pigments in medieval book arts. Azurite can be seen in the blue regions such as the robe of the praying figure, the sky, and blue decorative elements in the border, while malachite was used for the green foliage and green marginal motifs. Image is in the public domain; source: The British Library (public domain via Wikimedia Commons); (right) Neoclassical malachite obelisks (19th century), reflecting the use of this copper carbonate hydroxide mineral in Russian decorative arts. The swirling green banding patterns are characteristic of polished malachite, and the gold double-headed eagle emblems highlight its ceremonial application. Image is in the public domain; source: Metropolitan Museum of Art (public domain via Wikimedia Commons).

Investigations carried out on prominent archaeological sites such as Xi'an, Pompeii, and Vienna have shown that there is substantial evidence that azurite and malachite have been present as a coating on copper and copper alloy objects. The archaeological studies carried out on various objects have shown that beads, plaques, decorative objects, and wires have been found with a thin layer of azurite and malachite [18]. The wooden objects from the Tang Dynasty, which were retrieved from the tomb of Princess Yongtai, were found to have pigments containing both azurite and malachite [18]. The azurite and malachite present on the objects from archaeological sites have been formed by slow chemical reactions between water containing dissolved carbon dioxide and organic acids and copper alloy objects over a long period [19]. The chemical reactions between water containing carbon dioxide and copper alloy objects produce a series of chemical compounds that result from the interaction between copper and carbon dioxide, which is present in water [19]. The initial compound that is formed is copper oxide (Cu_2O), which is followed by the formation of a series of basic copper carbonates and copper sulfates that result from the interaction between copper and carbon dioxide, sulfur oxides, and chloride ions that penetrate the burial environment [19]. The final product that is formed is a stable compound of copper, i.e. malachite ($Cu_2CO_3(OH)_2$), which is a green mineral that protects the object from any further chemical reactions [19]. The chemical product that is formed on copper objects is a mixture of copper and other chemical compounds that have been formed over a long period.

A major challenge for modern heritage science is that the artifacts with these archaeological and artistically important corrosion products and pigment materials demand fast and non-destructive analytical techniques with the ability to analyze the spatial distribution of minerals and their chemical stability for appropriate conservation treatment. Destructive sampling of unique artifacts is not only unethical but also scientifically not desirable, as it involves the loss of irreplaceable material evidence [20]. Instead, a set of non-invasive and minimally invasive

How to cite this article:J Theo Kloprogge. The Use of X-Ray Photoelectron Spectroscopy in Studying Azurite and Malachite as Minerals, Pigments and in Secondary Products on Copper Objects. JOJ Material Sci. 2026; 10(3): 555788. DOI: 10.19080/JOJMS.2026.10.555788

spectroscopic techniques has been developed and increasingly employed to characterize complex minerals and corrosion products in their original context.

Fourier Transform Infrared Spectroscopy (FTIR) has been employed as an important tool for identifying the characteristic vibrational modes of azurite, malachite, and other copper minerals [21,22]. FTIR, which can be used in both portable and laboratory versions, has been employed to identify and distinguish between azurite and malachite on the basis of characteristic vibrational bands in the IR spectrum. Azurite has been identified by characteristic bands in the carbonate and hydroxide regions of the spectrum, while malachite has been identified by a similar but distinctive vibrational pattern [11,22]. FTIR has been particularly useful for identifying natural and synthetic differences between these minerals [23] and for identifying degradation products of these minerals that occur upon aging and/or conservation treatments [24]. The ATR (Attenuated Total Reflection) and DRIFT (Diffuse Reflectance Infrared Fourier Transform) versions of FTIR spectroscopy have been found to be effective for identifying historical pigments [25]. DRIFT spectroscopy has been particularly useful for in-situ, portable spectroscopic analysis of unknown materials in the field, which makes it particularly useful for evaluating the conditions of archaeological sites [22]. A database of FTIR spectra of historical pigments such as azurite and malachite has been developed to enable the rapid identification of unknown materials [22].

Raman Spectroscopy, in its portable, micro-scale, and micro-SORS (Spatially Offset Raman Spectroscopy) forms, is capable of offering supplementary molecular information, thereby aiding in the comprehensive characterization of mineral phases present in complex multilayered paint systems and corrosion crusts [26]. Raman spectroscopy has been effectively used to differentiate between azurite and malachite on the basis of their Raman vibrational bands, where the Raman spectrum for each mineral phase is unique [9-11, 21]. More in-depth Raman studies have also been able to identify the asymmetric and symmetric stretching vibrations of the carbonate anion, in addition to resonance Raman features due to Cu (II) transitions [27]. This is particularly useful in identifying degradation products, which may be present in addition to the original mineral phases. Portable Raman spectrometers have been effectively used in the analysis of medieval illuminated manuscript paintings, where Raman spectra were able to identify the presence of azurite and malachite pigments, in addition to other pigments, thereby showing its potential in the non-destructive analysis of original works of art [28]. The high spatial resolution offered by Raman spectrometers, in particular, allows for the mapping of distinct pigment domains in complex multilayered paint systems, thereby revealing the complex use of pigments and binders in works of art created over the ages [29]. Raman mapping techniques have also been used in the non-destructive analysis of complex mural paintings, where the distribution of pigments, in addition to identifying degradation products and conservation materials, has been characterized [26]. The recent advent of micro-SORS spectrometers has also enabled Raman spectrometers to non-destructively probe complex works of art, where layers may be present beneath the surface, due to subsequent restoration or mechanical damage [30,31].

X-ray Photoelectron Spectroscopy, although requiring the removal of a small sample (milligrams or less), offers unparalleled chemical information, including the ability to determine the oxidation state of elements, the composition of the material, and the shift in the binding energy, which can be used to diagnose the presence of particular mineral phases and their degradation mechanisms. Although a laboratory technique requiring the transportation of the sample, the ability of XPS to determine the oxidation state of copper, whether Cu^{+} or Cu^{2+}, and the ability of the technique to determine the presence of surface-enriched degradation products make the technique invaluable for the investigation of the corrosion mechanisms of archaeological copper and bronze objects. In addition, the ability of the technique, with the use of depth profiling, to determine the compositional changes through the patina layers, which are directly related to the environmental history of the artifact, makes the technique particularly useful for the investigation of the history of the artifact [20].

Complementary techniques, like X-ray fluorescence spectroscopy (XRF), which helps determine the elemental composition of a material, X-ray diffraction (XRD), which helps determine the crystalline mineral composition, and scanning electron microscopy with EDS (Energy Dispersive X-ray Spectroscopy), which helps determine the microstructure of a material, provide important supplementary information, as suggested by [20]. This multi-technique approach, employed through a series of protocols from initial rapid and portable techniques like portable Raman and portable XRF, to subsequent in-depth analysis like micro-FTIR, micro-Raman, XRD, SEM-EDS, and XPS, helps ensure a comprehensive analysis of the archaeological and artistic objects without compromising the ethics of minimal intervention, as suggested by [20]. By correlating the chemical data obtained from the various spectroscopic and microscopic techniques with historical, archaeological, and artistic information, important insights into the ancient manufacturing and trade practices, and restoration and preservation strategies, are provided, as suggested by [20].

Methodological Foundation

X-ray photoelectron spectroscopy (XPS) is an essential analytical technique for the study of the surfaces of copper-bearing minerals and their derivatives. This technique is of profound significance in the study of the flotation of ores and the conservation of cultural heritage. XPS is a powerful tool for gaining vital knowledge about the chemical composition of the surfaces of azurite and malachite at the nanometer scale [32]. However, the analysis of the surfaces of these two compounds using XPS is a challenging task. This review critically examines the findings from the XPS analysis of the surfaces of the two compounds in order to

How to cite this article: J Theo Kloprogge. The Use of X-Ray Photoelectron Spectroscopy in Studying Azurite and Malachite as Minerals, Pigments and in Secondary Products on Copper Objects. JOJ Material Sci. 2026; 10(3): 555788. DOI: 10.19080/JOJMS.2026.10.555788

understand the strengths and weaknesses of the technique in the analysis of the compounds.

XPS Characterization of Azurite and Malachite as Primary Minerals

The pioneering XPS work on the chemical composition of azurite ($Cu_3(CO_3)_2(OH)_2$) and malachite ($Cu_2CO_3(OH)_2$) minerals has been largely driven by flotation research with the aim of enhancing the efficiency of recovery and separation of these minerals and other gangue minerals. Such research has clearly demonstrated that XPS has been highly effective in identifying the surface chemical states and adsorption mechanisms of flotation collectors on these minerals. In a recent study on a novel thiophosphate-based collector, namely dibutoxy-thiophosphorylsulfanyl-acetic acid (CDDP), for instance, it was demonstrated that this new collector had enhanced collecting efficiency on the surfaces of azurite, with evidence obtained by XPS that this new collector could easily chemically react with copper ions on the surface of the minerals [33]. Similarly, XPS results on the surfaces of azurite and malachite minerals treated with various phosphonic acid-based flotation collectors, namely BTPA, DEPA, and DPPA, demonstrated that the chemical adsorption characteristics of these collectors on the surfaces of these minerals could be clearly distinguished on the basis of the difference in binding energies, with charge transfer between oxygen atoms of the collectors and d orbitals of copper atoms identified as the key factor for adsorption strength [34].

The strength of the mineral-focused XPS studies lies in the level of detail provided for the analysis of surface reactivity and complex chemical interactions. However, a major limitation of the studies becomes apparent when considering the purity and homogeneity of the mineral samples used for the analysis. Natural azurite and malachite samples often contain trace amounts of various elemental impurities, such as lead, zinc, arsenic, cadmium, manganese, and uranium, depending on the geological source of the mineral, as identified by [35]. In the case of XPS analysis of natural mineral samples without considering the presence of impurities, the overall shape of the X-ray photoelectron spectra might be affected not only by the presence of the carbonate and hydroxide phases but also by the presence of secondary mineral phases and impurities on the surface of the mineral particles.

Azurite and Malachite as Historical Pigments: Distinct Compositional and Surface Characteristics

The shift from viewing azurite and malachite as ore minerals to viewing them as historical pigments adds substantial complexity to the interpretation of the data obtained from the XPS analysis. The historical pigments of azurite and malachite exhibit changes in composition related to the geological source of the mineral ore and the processing techniques used by the artists [35]. The historical pigments of azurite and malachite may include adventitious malachite as an impurity in the azurite pigments, which plays an important role in determining the elemental composition of the sample obtained from the XPS analysis. For example, the elemental composition of the azurite pigments obtained from the ore deposits of Central Europe exhibits characteristic fingerprints of the presence of lead and rare earth elements, but the presence of increased malachite as an impurity in the azurite pigments changes the elemental composition of the sample considerably. This is a fundamental problem in the interpretation of the data obtained from XPS analysis, as the data obtained from a single analytical technique cannot easily distinguish between the primary pigments and secondary minerals present in the sample if the surface chemistry is similar [35].

XPS analysis has also revealed that, in terms of surface chemistry, both azurite and malachite experience significant changes due to their exposure to photochemical and thermal degradation. The pigments were exposed to ultraviolet radiation, causing considerable variations in the transmittance spectra and elemental composition, with azurite showing greater changes in terms of color, even if the changes in the spectra were not so significant compared to malachite, suggesting that changes in composition do not necessarily result in changes in color, thereby emphasizing the need for correlation between XPS analysis and other analytical tools [24].

Comparative Analysis: Mineral, Pigment, and Corrosion Product Distinctions

One of the critical difficulties associated with interpreting XPS results for azurite and malachite samples is that the same chemical formula can have dramatically different surface chemistry. The pristine surfaces of synthesized azurite and malachite minerals used for flotation studies have well-defined Cu^{2+} oxidation state features and characteristic carbonate-hydroxide-related O1s features [33], while azurite and malachite pigments from a historical context may have partially degraded, variable composition, and variable composition from substrates or binding media Figure 3. The copper corrosion products that form on exposed copper surfaces, including cuprite (Cu_2O), brochantite ($Cu_4SO_4(OH)_6{\cdot}2H_2O$), atacamite ($Cu_2Cl(OH)_3$), and copper oxide-sulfide combinations, also have very different oxidation state compositions when analyzed by XPS. The XPS analysis of the corrosion products that formed on copper exposed to hot spring environments has been determined to be a mixture of Cu_2O and Cu_2S with a difference in copper chemical state in the uppermost surface region, which would appear qualitatively similar to degraded azurite or malachite samples but is fundamentally different from their formation mechanisms [36].

Architectural Copper and Patina Formation: Complexity of Field-Exposed Surfaces

The nature of the XPS problem for architectural copper and copper alloys is arguably the most challenging of any of the XPS applications thus far. The heterogeneous, multi-layer nature of the corrosion products on architectural copper and its alloys is the

How to cite this article:J Theo Kloprogge. The Use of X-Ray Photoelectron Spectroscopy in Studying Azurite and Malachite as Minerals, Pigments and in Secondary Products on Copper Objects. JOJ Material Sci. 2026; 10(3): 555788. DOI: 10.19080/JOJMS.2026.10.555788

cause of the problem. The natural patina that develops on copper exposed in urban, rural/coastal, and hot spring environments has been found to have distinctly different phase compositions. In urban and rural/coastal environments, the composition is hydrated sulfate and cuprite, while the hot spring environment, which is dominated by H_2S, has Cu_2S-rich corrosion products [37]. The identification of the composition of the corrosion products on architectural copper and its alloys is complicated by a number of factors. The nanometer-scale spatial variability of composition is one factor. The presence of sulfur, chlorine, and other contaminants is another factor that contributes to the complexity of the XPS problem. The time-dependent nature of the transformation of primary corrosion products into secondary phases is also a factor. For example, the initial corrosion product formed on copper exposed in urban environments is posnjakite, which is converted into brochantite during extended exposure. However, the composition of posnjakite and brochantite is identical: Cu^{2+} and sulfate [37].

The artificial patination of copper by exposure to humid environments containing SO_2 has been studied, and the development of the patina has been monitored kinetically by XPS, confirming the formation of brochantite [38]. However, the question of the relevance of the XPS data from the artificial patination of copper, which yields a more homogeneous and chemically well-defined patina, to the naturally aged copper surfaces must be addressed. A parallel question of relevance arises from the comparison of the XPS data from the artificial and natural aged azurite/malachite pigment surfaces and the copper surfaces: the relevance of the XPS data from a single point on a copper roof or copper sculpture, exposed to the atmosphere, to the overall composition of the patina on the copper surface, owing to the variability of the microenvironment.

Oxidation State Quantification and Binding Energy Assignments with Detailed Analysis of Crystal Structure Effects, Chemical Reactions, and Thermal Degradation

One of the most important considerations for XPS analysis of these copper materials is the identification of the oxidation states of the copper, the identification of the binding energies of the photoemitted electrons with the chemical species of interest, and the identification of how the binding energies are related to the crystal structure of the material. The photoemission spectrum of copper is complex due to multiple splitting caused by the interaction of the photo hole and the unpaired d electrons. The binding energies of the core electrons for copper are highly dependent on the local environment, oxidation state, and structure of the material. XPS is a useful technique for identifying different phases of copper. However, for proper identification, knowledge of how the binding energies change with structure is necessary.

Binding Energy Values and Crystal Structure Relationships

The fundamental Cu $2p_3/2$ binding energies of the azurite and malachite are of great importance in the understanding of the relationship between the crystal structure of the materials and the resulting photoemission spectra. From the Handbook of Mineral Spectroscopy by [39], azurite, with the chemical composition $Cu_3(CO_3)_2(OH)_2$, has a primary Cu $2p_{3/2}$ peak at 934.6 eV corresponding to the Cu^{2+} ion, with characteristic shake-up satellite structures at 940.3 eV and 943.6 eV corresponding to the final state of the Cu^{2+} ion, resulting from the interaction of the photo hole and the unpaired d-electrons of the ion [40,41]. The oxygen 1s core-level spectrum of the azurite mineral has distinct peaks at 531.4 eV corresponding to the carbonate ion and at 532.1 eV corresponding to the hydroxyl ion, resulting from the trigonal pyramidal coordination of the copper ion in the monoclinic crystal structure of the mineral. The carbon 1s core-level spectrum of the mineral has a primary peak at 289.3 eV corresponding to the carbonate ion, with the theoretical value of the atomic percentage being 15.4%, while the experimental value is 13.8%, giving a Cu:C ratio of 2.4:2.0 [40]. The minor differences between the theoretical and experimental values of the atomic percentages are attributed to the surface-sensitive nature of the XPS technique and the presence of impurities such as sodium and silicon in the sample.

In contrast, for malachite, $Cu_2CO_3(OH)_2$, with its different crystal structure and layer stacking and coordination environments for copper, a very distinct XPS spectrum is observed. The dominant Cu $2p_{3/2}$ peak is observed at a binding energy of 935.1 eV for Cu^{2+}, a value that is shifted by approximately 0.5 eV from that observed for azurite at 934.6 eV, a very small but extremely critical difference that is directly indicative of the unique coordination environment around copper in each compound [40,41]. Although a small binding energy shift is observed, such a value is easily measurable with modern XPS analysis techniques and is critical for differentiation between these two copper carbonates, even when present as a mixture or degradation product in an artifact.

One of the most remarkable and significant findings that are evident from the Handbook data is the presence of Cu^+ in the malachite sample, indicated by the presence of a Cu $2p_{3/2}$ peak at 932.9 eV, along with the main Cu^{2+} peak at 935.1 eV [40]. The Handbook explicitly states that "a small amount of the copper in malachite changed from Cu^{2+} to Cu^+ under the X-rays of the XPS instrument." This is an important phenomenon that is of critical interest while interpreting XPS results for copper-containing minerals and pigments. This finding shows that an apparently pure and well-ordered malachite mineral is capable of undergoing partial redox transformations during XPS analysis owing to the X-ray energy employed. This indicates that the XPS results obtained are for a mixed oxidation state of copper, derived from

How to cite this article: J Theo Kloprogge. The Use of X-Ray Photoelectron Spectroscopy in Studying Azurite and Malachite as Minerals, Pigments and in Secondary Products on Copper Objects. JOJ Material Sci. 2026; 10(3): 555788. DOI: 10.19080/JOJMS.2026.10.555788

what is theoretically a pure Cu^{2+}containing mineral. The Cu^{+} peak is found at 932.9 eV, along with satellite peaks at 938.9 eV, 941.7 eV, and 943.9 eV [40]. This is an important finding that serves to underscore the importance of standardization of XPS results. The presence of mixed Cu(I) and Cu (II) states in what is theoretically a pure Cu (II) state is an important indicator of the complexity of real samples and the potential for photo-induced reduction during XPS analysis. The photo-induced reduction phenomenon has significant implications for the interpretation of aged pigments and archaeological samples, where such transformations may have occurred during or after analysis.

The carbon 1s region in malachite is also more complex compared to that in azurite, with the carbonates having a peak at 289.2 eV, the carbon in the C-O bond having a peak at 286.3 eV, and the reference peak at 294.8 eV [40]. The peak at 286.3 eV is attributed to carbon in the C-O bond, which may indicate the existence of variations in the bonding environment compared to the carbonates. The oxygen 1s region in malachite also shows peaks at 531.3 eV, attributed to carbonates, and at 532.0 eV, attributed to hydroxyl groups, with an additional peak at 532.9 eV attributed to O-C [40]. The atomic composition in malachite is also very different from the calculated composition, with the measured Cu at 14.0% compared to the calculated 25.0%, the measured C at 13.4% compared to the calculated 12.5%, and the measured O at 34.9% compared to the calculated 37.5% for carbonates [40]. These larger variations may be attributed to the surface sensitivity of the XPS technique, as well as the presence of Si-based silicates, which were also present in very small amounts in the sample.

The difference between Cu(I) and Cu (II) becomes significant when analyzing the composition of aged pigments or corrosion products, as suggested by [42]. In fact, the Handbook's evidence of coexisting Cu^{+} and Cu^{2+} in a single sample of malachite, measured at 932.9 and 935.1 eV, respectively, provides a useful reference standard for peak fitting of Cu 2p spectra in more complex samples. Pure Cu(I) oxide, Cu_2O, has a Cu $2p_{3/2}$ core level with a binding energy of 932.5-933.0 eV [42] placing it at or very near the Cu^{+} position of 932.9 eV measured for the malachite pigment sample analyzed by [39]. By comparison, the Cu (II) oxide, CuO, has a Cu $2p_{3/2}$ core level measured at 933.8-934.0 eV, and the pure Cu (II) in hydroxide or carbonate has a Cu $2p_{3/2}$ core level measured at 934-935 eV, as suggested by the Handbook and recent literature [40,43]. In the case of a mixture of Cu(I) and Cu (II) oxidation states, coexisting in a corroded surface or on a particle of aged pigment, the Cu 2p photoemission spectrum will be a composite of the two features. For accurate analysis, the use of high-resolution spectra of reference materials, like those provided in the Handbook of Mineral Spectroscopy, makes peak fitting with reference standards a necessary step for accurate analysis. In fact, in many historical pigment and archaeological material samples, Cu(I) and Cu(II) are expected to coexist, and for example, in the case of the aged surface of a sample of the pigment azurite, Cu(II) carbonate, some Cu(I) might be present, resulting from a degree of reduction and/or photochemical alteration of the Cu(II) component, making the analysis particularly difficult, as suggested by [44] Table 1.

Table 1: Comparative XPS Data for Azurite and Malachite from High-Resolution Spectroscopy.

Element	Peak Type	Binding Energy (eV) - Azurite	Binding Energy (eV) - Malachite	Assignment	Atom% Azurite (Measured)	Atom% Malachite (Measured)
Cu $2p_{3/2}$	Primary	934.6 (Cu^{2+})	935.1 (Cu^{2+}); 932.9 (Cu^{+})	Copper oxidation state	9.6	1.2 (Cu^{+}); 6.5 (Cu^{2+})
Cu $2p_{3/2}$	Satellite 1	940.3	938.9	Shake-up structure	3.2	1.6
Cu $2p_{3/2}$	Satellite 2	943.6	941.7; 943.9	Shake-up structure	3.7	2.3; 2.3
C 1s	Primary	289.3	289.2	Carbonate carbon (CO_3)	13.8	5.7
C 1s	Secondary	—	286.3	C-O species	—	7.7
C 1s	Reference	—	294.8	Reference/adventitious carbon	—	27.2
O 1s	Primary	531.4	531.3	Carbonate oxygen (CO_3)	55.7	21.8
O 1s	Secondary	532.1	532	Hydroxyl oxygen (OH^{-})	13.9	13.1
O 1s	Tertiary	—	532.9	O-C species	—	10.6
Elemental Ratio	Cu:C:O	2.4:2.0:8.1	2.5:1.0:6.1 (Cu^{2+}); Variable (Cu^{+})			

Source: Kloprogge and Wood [40], Handbook of Mineral Spectroscopy Volume 1: X-ray Electron Spectra. Note: Azurite theoretical formula $Cu_3(CO_3)_2(OH)_2$; Malachite theoretical formula $Cu_2CO_3(OH)_2$. Trace amounts of Na and Si present as impurities in both samples. The presence of Cu^{+} in malachite was attributed to photo-induced reduction during XPS measurement.

How to cite this article:J Theo Kloprogge. The Use of X-Ray Photoelectron Spectroscopy in Studying Azurite and Malachite as Minerals, Pigments and in Secondary Products on Copper Objects. JOJ Material Sci. 2026; 10(3): 555788. DOI: 10.19080/JOJMS.2026.10.555788

Photo-Induced Reduction: A Critical Consideration for XPS Analysis of Copper Minerals

The observation of Cu^{+} generation in malachite during XPS measurement, as observed by Kloprogge and Wood [40], is an especially notable phenomenon that requires a detailed discussion. The phenomenon of photo-induced reduction, where Cu^{2+} is partially reduced to Cu^{+} by X-rays used during XPS measurement, is an especially notable phenomenon with important implications for understanding spectroscopic data from copper-bearing minerals and archaeological objects. Although the handbook specifies that "a small amount of the copper in malachite changed from Cu^{2+} to Cu^{+} under the X-rays of the XPS instrument," a discussion of the extent and mechanisms involved is necessary [40].

There are several possible mechanisms for the photo-induced reduction in XPS. Firstly, the X-ray used in XPS, with a typical energy of 1.487keV for Al Kα or 1.254keV for Mg Kα, has sufficient energy to produce, in addition to the initial photoelectrons, secondary electrons, Auger electrons, and other energetic particles within the sample. If the sample contains carbonaceous or reducible matter, then the conditions for reduction are locally produced. In the case of the mineral malachite, the presence of the carbonate ion, with carbon in the +4-oxidation state and inherently susceptible to electron transfer, might provide pathways for the electron transfer, resulting in the reduction of Cu^{2+} ions to Cu^{+} ions. That the Cu^{+} ions are produced "under the X-rays," as suggested by the handbook, implies a dynamic and ongoing process during the XPS measurement, and not a static condition in the pristine mineral sample [40].

The amount of photo-induced reduction present in the malachite sample was relatively small but not insignificant. As demonstrated by the handbook data, there was a measured Cu^{+} peak present with 1.2% atomic percentage, appearing alongside 6.5% Cu^{2+} in the same measurement, indicating that approximately 15.6% of the copper atoms present had been reduced to the +1 state (calculated as 1.2/ (1.2+6.5) = 0.156 or 15.6%) [40]. Although this represents a minority of the total copper present, it is significant enough to be readily identifiable in high-resolution spectra. The fact that Cu^{+} and no other reduced species (such as metallic Cu^{0}) are produced indicates that this process is controlled and limited in some way, likely due to kinetic factors and/or the availability of appropriate electron-accepting sites in close proximity to the Cu^{2+} centers under measurement.

The implications of photo-induced reduction are considerable. In analyzing aged azurite and malachite pigments from paintings and other objects, XPS analysts must be aware that, to some degree, the detected Cu^{+} levels are not necessarily due to real compositional changes but might have occurred due to photo-induced effects. It is not easy to differentiate between these two effects. However, there are several options to reduce this uncertainty: (1) to carry out XPS analysis using different X-ray sources (Al Kα and Mg Kα) and varying X-ray flux intensities to investigate the effect of photon dose on Cu^{+} photo-reduction; (2) to use lower X-ray energies and shorter analysis times per specific sampling area to reduce the total dose of X-rays absorbed by the sample; (3) to apply other analytical methods, e.g., electron paramagnetic resonance spectroscopy, which detects Cu^{2+} but not Cu^{+}, and X-ray diffraction, which detects Cu_2O but not Cu^{+}; and (4) to measure several samples of the same material, including fresh and aged materials, to determine a reference photo-reduction rate, which can be subtracted from the total detected amount [40].

The data presented in the handbook also demonstrates a subtle point with respect to the standardization of reference spectra, namely, if the reference material used for Cu (II) analysis, namely, the mineral malachite, is used without correcting for the formation of Cu^{+} from Cu^{2+} due to the X-ray exposure, then incorrect Cu^{+} peaks would be introduced into the reference spectra, resulting in errors for unknown spectra. This demonstrates the importance of either: a) the use of reference materials measured under specified conditions of X-ray flux and exposure, or b) the use of calculated values of the binding energies, typically from high-level quantum chemical calculations, for mineral systems. The documentation of the observation of the photo-reduction of Cu^{2+} to Cu^{+} in the handbook provides a useful reference for the expected baseline behavior of the mineral, particularly for the case of the mineral malachite [40].

Comparative Spectral Features: Complex Overlapping Signals and Structural Distinctions

Apart from the major binding energy values for the Cu_2p level, an in-depth investigation of the carbon and oxygen levels shows significant structural and compositional differences between azurite and malachite that further emphasize the impact of crystal structure on XPS spectra. Although both are copper carbonate minerals, the difference in their crystal structure results in measurable differences in their photoemission spectra for chemically similar species [40]. This comparison is vital to understanding how XPS can identify differences between minerals and their alteration products.

A comparison of this type is particularly instructive. For azurite, there is a clear and distinct primary peak at 289.3eV due to carbonate carbon. In addition, there is excellent agreement between the atomic percentage calculated from this XPS measurement (13.8%) and the theoretically calculated stoichiometry (15.4%). This gives a Cu:C ratio of 2.4:2.0, or 1.2:1 [40]. The simplicity of this XPS spectrum reflects the crystal structure of azurite, where there are no differences in crystal sites occupied by carbonate. In stark contrast, there are three peaks in the carbon 1s XPS spectrum of malachite: a main carbonate

How to cite this article: J Theo Kloprogge. The Use of X-Ray Photoelectron Spectroscopy in Studying Azurite and Malachite as Minerals, Pigments and in Secondary Products on Copper Objects. JOJ Material Sci. 2026; 10(3): 555788. DOI: 10.19080/JOJMS.2026.10.555788

carbon peak at 289.2eV, similar to azurite. In addition, there are peaks due to C-O at 286.3 eV and adventitious carbon at 294.8eV. The atomic percentage values calculated from these peaks (5.7%, 7.7%, and 27.2%, respectively) are considerably different from those calculated from the stoichiometry of $Cu_2CO_3(OH)_2$.

The appearance of the C-O peak at 286.3 eV in malachite but not azurite is particularly interesting. This C-O peak is likely associated with carbon atoms bonded directly to oxygen and is not characteristic of a simple carbonate (CO_3^{2-}) group. The C-O peak may be associated with: (1) bridging carbonates that coordinate to multiple copper centers, thereby weakening the C-O bonds and resulting in a lower binding energy value; (2) partially degraded carbonates; or (3) defects or disorders present in the malachite lattice [40]. The C-O peak observed at 286.3eV is significantly lower in binding energy compared to the main peak corresponding to a carbonate group at 289.2 eV, with a difference of 3.0eV. This is a very electron-rich environment compared to the environment associated with the main peak corresponding to a carbonate group. The carbon atom associated with the C-O peak is therefore experiencing a much weaker electrostatic attraction to its nucleus compared to a carbon atom associated with a carbonate group.

The oxygen 1s spectra also support this analysis of structural complexity in malachite. The oxygen spectra for azurite consist of only two oxygen environments: one corresponding to oxygen from carbonates at 531.4 eV and a second corresponding to oxygen from hydroxyls at 532.1eV, with measured percentages of 55.7% and 13.9%, respectively, which is very close to the theoretical ratio expected for a $Cu_3(CO_3)_2(OH)_2$ formula (theoretical oxygen 1s: 46.2% for CO3 and 15.4% for OH) [40]. The measured oxygen percentages being slightly above theoretical (55.7% measured, 46.2% theoretical) is attributed to the higher ionization cross section for oxygen and the presence of small amounts of impurity phase silicates that were also present in the sample. The oxygen spectra for malachite consist of three oxygen environments: a peak corresponding to oxygen from carbonates at 531.3eV (21.8%), a second corresponding to oxygen from hydroxyls at 532.0eV (13.1%), and a third corresponding to a tertiary O-C bond at 532.9 eV (10.6%) [40]. The presence of a third oxygen peak at 532.9eV is again unique to malachite and suggests that some oxygen is present in a bonding environment that is neither simply carbonates nor hydroxide, which is consistent with the C-O bond observed in the carbon spectrum.

These specific spectral variations between azurite and malachite serve to illustrate an important general principle in the interpretation of XPS spectra, whereby minerals with ostensibly similar chemical composition and identical initial oxidation states may show significant variations in their XPS spectra, depending on variations in crystal structure. The spectra provided in the handbook serve to illustrate this point, in that variations in crystal structure are seen to affect not only the principal features of element-specific spectra but also the fine detail, satellite features, and the presence of subsidiary peaks corresponding to alternative bonding configurations [40].

Additionally, the discrepancies in the theoretical and calculated percentages for the elements in both minerals, especially in malachite, underscore the sensitivity of the technique to the surface layer of the sample and the effect of heterogeneity in the sample. It is stated in the handbook that Na and Si impurities in the mineral are present in the form of silicates. However, the large discrepancies in the calculated and actual percentages indicate the possibility of other factors influencing the XPS spectra, such as the segregation of elements to the surface layer of the sample. This is especially true for the Cu content in malachite, which is significantly lower in the actual measurement (1.2%) than in the calculated percentages (25.0%), indicating the possibility of the surface layer being depleted in Cu content relative to the bulk phase of the mineral. This type of analysis does not only show the chemical composition of the mineral but also its reactivity.

Binding Energy Changes During Corrosion and Patina Formation

The formation of patinas on copper surfaces exposed to the environment is characterized by changes in the oxidation states and chemical environment of copper, which is observable using XPS analysis and understanding the changes in binding energies during the degradation process Figure 3. During the initial corrosion process, metallic copper (Cu^0) is converted to Cu_2O (cuprite). The Cu 2p core level spectrum is characterized by binding energies around 932.5eV [45]. The XPS analysis on copper surfaces exposed for long durations in different atmospheric conditions showed that during the initial stages, cuprite is the dominant corrosion product, where copper in Cu_2O has a lower binding energy compared to Cu (II). When copper is exposed to the atmosphere for long durations, the corrosion products gradually change due to the presence of sulfur dioxide in the atmosphere. During this period, copper is converted from Cu_2O to brochantite ($Cu_4SO_4(OH)_6 \cdot 2H_2O$). The Cu (II) in brochantite is characterized by binding energies ranging from 934-935eV, showing an increase in the copper oxidation state, similar to the binding energies in the azurite and malachite minerals, as discussed in the literature by Kloprogge & Wood [40].

A particularly illustrative case of the evolution of binding energies during the process of corrosion can be exemplified by the depth profiling of multi-layered systems of patina. In the urban atmospheric environment with mixed acid rain-induced acceleration of the corrosion process, the top layer of the patina contains Cu (II)-based compounds such as sulfates, oxides, and hydroxy oxides. In the interfacial region of the corrosion product layer and the underlying Cu metal, Cu_2O is found to be favored. In the XPS depth profiling of such multi-layered systems of the patina, the binding energy shifts are found to be indicative of the position of the Cu species in the layered structure. Lower binding energies

How to cite this article:J Theo Kloprogge. The Use of X-Ray Photoelectron Spectroscopy in Studying Azurite and Malachite as Minerals, Pigments and in Secondary Products on Copper Objects. JOJ Material Sci. 2026; 10(3): 555788. DOI: 10.19080/JOJMS.2026.10.555788

at the metal-oxide interface (~932eV) correspond to Cu(I). In the top layer of the corrosion product layer, higher binding energies (~934 to 935eV) are indicative of Cu (II) in the forms of Cu sulfate and Cu hydroxy carbonate. The gradient in the binding energy in the single layer of the patina thus provides direct evidence of the oxidation-reduction gradients in the atmospheric corrosion process. The binding energies in the corrosion layer are similar to the reported values by Kloprogge & Wood [40] for malachite (~935.1 eV for Cu^{2+} in malachite) and for the partially reduced malachite (~932.9eV for Cu^{+} in the reduced malachite).

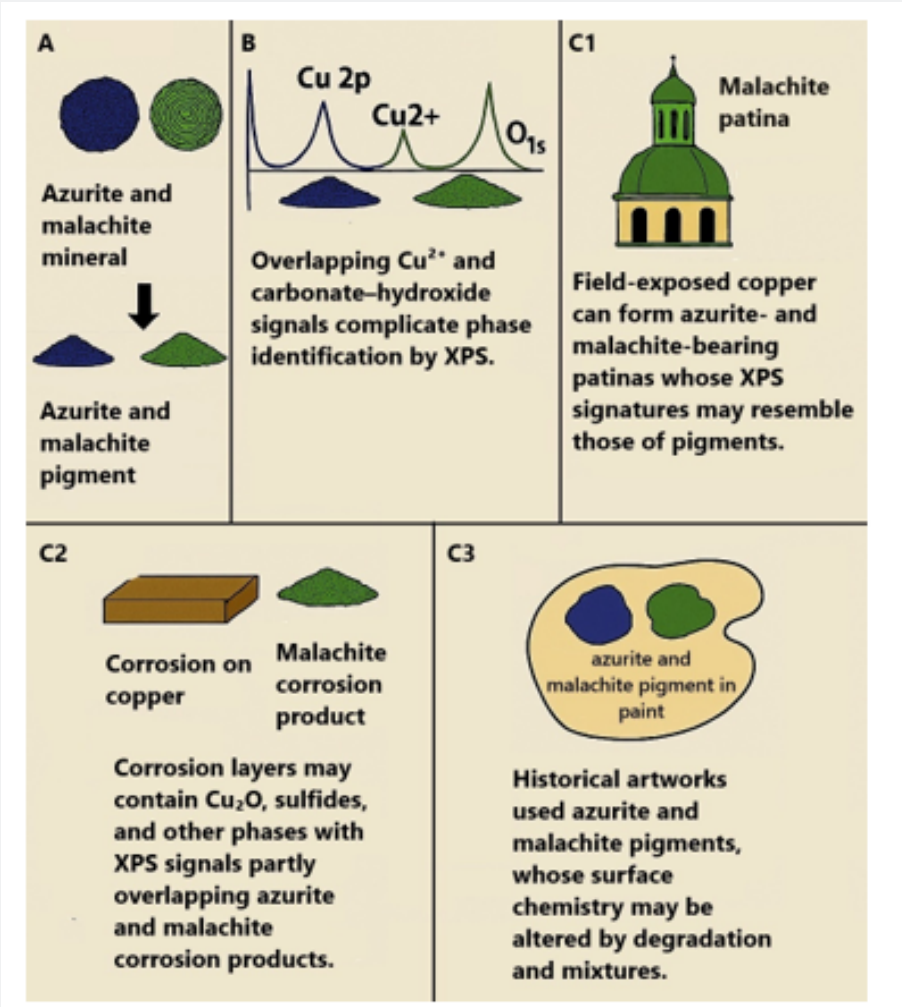

Figure 3: Distinct XPS signatures of azurite and malachite across mineral, pigment, and patina contexts. (A) Azurite and malachite minerals transformed into historical pigments exhibit compositional variability due to impurities and processing history. (B) Comparative XPS spectra of azurite, malachite, and copper corrosion products show overlapping Cu^{2}□ and carbonate-hydroxide signals, complicating phase identification based on Cu 2p and O 1s regions. (C) Patina and corrosion contexts illustrate how malachite patinas (C1), malachite corrosion products (C2), and azurite–malachite pigment mixtures can produce XPS signatures that resemble one another, especially in field-exposed or degraded surfaces (C3).

In the presence of hydrogen sulfide in hot spring environments, the chemistry of the corrosive process changes considerably. In this case, the major corrosion products are Cu 2S, known as chalcocite, where copper has an oxidation state of +1 and has lower binding energies [46]. In cases where both Cu_2O and Cu_2S are present on the same corroded surface, as has been noted in environments with mixed chemistry, it has been established that the distinction between these two compounds can be made by closely examining the Cu2p spectrum, where there are slightly differing satellite features and peak shape for the presence of Cu_2S compared to Cu_2O [46]. The binding energies for the Cu^{+} in the three compounds, namely Cu_2O, Cu_2S, and the photo-reduced malachite phase identified by Kloprogge & Wood [40] and having a binding energy of 932.9eV, fall in a narrow range of approximately 932.0 to 933.5eV.

How to cite this article: J Theo Kloprogge. The Use of X-Ray Photoelectron Spectroscopy in Studying Azurite and Malachite as Minerals, Pigments and in Secondary Products on Copper Objects. JOJ Material Sci. 2026; 10(3): 555788. DOI: 10.19080/JOJMS.2026.10.555788

Binding Energy Changes During Thermal Degradation and Decomposition

Thermal degradation of the azurite and malachite pigments involves sequential oxidation-reduction reactions, which result in specific and measurable changes in the binding energies Figure 3. The specific binding energies for these pigments, provided in the study by [40], serve as an initial basis for understanding the impact of thermal degradation on these minerals. The thermal degradation process for the copper pigments, when subjected to increasing temperatures, initially involves dehydration at temperatures less than 200°C, which may result in specific Cu 2p binding energy changes due to the alteration in the hydroxide coordination environment around copper [47]. At temperatures between 200-300°C, the copper carbonates dehydroxylate, leading to structural changes in the compound. The XPS spectrum obtained from copper carbonates, which have been subjected to thermal degradation, indicates that during dihydroxylation, the Cu 2p binding energies change, reflecting changes in the coordination environment around copper, from hydroxide-rich to oxide-rich coordination [48]. At 300°C, copper oxide and copper carbonate may coexist, leading to complex XPS spectra, where multiple features may be present. The binding energies for these copper pigments at intermediate stages will be between the main features in the handbook spectra for the pure copper carbonates (934.6eV for copper in azurite and 935.1eV for copper in malachite) and the binding energies for CuO [48].

Further heating to 400°C and above leads to the complete transformation of azurite to tenorite (CuO) or malachite to a combination of tenorite and finally copper(I) oxide in a reducing environment [48]. The Cu $2p_{3/2}$ binding energy for the pure CuO phase is centered at 933.5 to 934.0eV, which is slightly lower than the Cu $2p_{3/2}$ binding energy for the hydroxycarbonate compounds. This is due to the absence of hydroxyl groups and the square planar coordination geometry of the Cu^{2+} ions in the CuO crystal. This Cu 2p binding energy for CuO at 933.5 to 934.0eV is significantly lower than the Cu^{2+} peak for malachite at 935.1eV and is even lower than the Cu^{2+} peak for azurite at 934.6eV [40]. This shows that the removal of the hydroxide ligand during the thermal decomposition leads to a decrease in the Cu 2p binding energy due to a reduction in the electrostatic potential around the Cu^{2+} ion. The presence of multiple Cu 2p peaks during the intermediate stages of heating, such as the simultaneous presence of Cu^{2+} from the carbonate and oxide compounds, makes the temperature-dependent XPS technique particularly useful for the study of the thermal decomposition of the compounds [47].

A crucial point of distinction arises in the case of the effect of the different electronegativities of the anion sites on the binding energies of the copper atoms in the minerals of interest [40]. The carbonate minerals of interest include azurite, with copper at 934.6 eV, and malachite, with Cu^{2+} at 935.1eV. The effect of the oxygen ligands of the carbonate CO_3^{2-} anions on the electron cloud of the copper atoms is naturally different from the effect of the hydroxyl OH^- ligands in the case of the malachite mineral or the oxide ligands of the O^{2-} anions present in the case of the cupric oxide mineral, with copper at 933.5-934.0eV. The shift in the Cu 2p binding energies of the malachite mineral, with Cu^{2+} at 935.1eV, and the CuO mineral, with copper at 933.5-934.0eV, can be as much as 0.5-1.6eV, demonstrating the fundamental shift in the electronic environment of the copper atoms during the thermal decomposition of the malachite mineral. The study of the changes in the binding energies of the copper atoms in the malachite mineral during the thermal decomposition process, carried out at increased temperatures, indicates that the changes in the binding energies of the copper atoms during the thermal decomposition of the malachite mineral are not static but occur in real-time during the thermal decomposition of the malachite mineral [49].

Multicomponent Systems and Quantification Challenges

In the case of partially degraded azurite and malachite pigments, the surface of the historical objects might be a mixture of the original pigment, partially degraded products, and secondary products of the degradation reactions. For instance, the partially degraded hydroxycarbonates might be present, and the secondary products might include tenorite and copper, resulting from the reduction of the copper ions in the presence of reducing agents. In the presence of a complex mixture of copper-containing components, the Cu 2p photoemission spectrum might be a convolution of the spectra of the individual components, each contributing copper with a different core-level binding energy. A good example of the complexity of the Cu 2p spectra of the mixed components, and the relevance of the handbook data, might be the observation of the coexistence of Cu^{2+} and Cu^+ in the same sample of the pigment, with Cu^{2+} present at a binding energy of 935.1eV and Cu^+ present at a binding energy of 932.9eV, as suggested by the handbook data for the pigment, according to the work of [40]. In the case of a quantitative analysis, the Cu 2p spectrum of the mixed components might be analyzed either by peak fitting, using reference spectra of the individual components, or by performing a depth profile analysis of the sample.

Peak fitting for such complex spectra can be particularly problematic, especially considering the potential for shake-up satellites associated with the Cu (II) species to fall into the binding energy range of the Cu(I) species. In this case, the handbook values are particularly useful, with the shake-up satellites for the azurite appearing at 940.3 and 943.6eV, and for malachite appearing at 938.9, 941.7, and 943.9eV [40]. These are considerably shifted from the binding energy of the Cu^+ peak (which appears at 932.9eV in the malachite spectrum). However, should there also be other peaks associated with other Cu (II) species with slightly shifted binding energies, or should there be other features associated with other elements (such as impurity elements with Auger features or other shake-up satellites), it should not always

How to cite this article:J Theo Kloprogge. The Use of X-Ray Photoelectron Spectroscopy in Studying Azurite and Malachite as Minerals, Pigments and in Secondary Products on Copper Objects. JOJ Material Sci. 2026; 10(3): 555788. DOI: 10.19080/JOJMS.2026.10.555788

be possible to separate the spectra to this extent. In fact, the best approach to this problem involves the acquisition of high-quality XPS spectra for pure azurite, pure malachite, pure Cu2O, pure CuO, and pure tenorite, and then performing a linear combination fit to the spectrum of the aged sample. Such an approach will only work effectively if it can be ensured that the reference spectra have been acquired under the same conditions of measurement (i.e., the same analyzer setting, pass energy, etc.) and under controlled X-ray flux to minimize any potential for photo-induced effects such as the reduction of Cu^{2+} to Cu^{+} that was noted by [40].

Binding Energy Shifts as Indicators of Charge Transfer and Interfacial Effects

Within composite materials or copper-containing pigments with multiple copper-containing phases in physical contact with one another, charge transfer between interfaces can occur and modify the binding energies beyond those expected for the individual phases (Wang et al., 2026). For example, in materials where both copper(I) oxide and copper (II) oxide are in physical contact, either through electrostatic or epitaxial interactions (which might occur in some degradation products or in composites synthesized for other purposes), the binding energies of the Cu2p peak might not reflect those of the pure phases due to charge transfer between copper(I) and copper (II) species. Such binding energies can give insight into the strength of interaction between phases and even whether there are any structural coherences between them. In the documentation of this handbook, for example, it has been noted that photo-induced formation of Cu^{+} occurs at a binding energy of 932.9eV in malachite [40]; if there are large changes in this binding energy for the Cu^{+} peak, this might reflect strong interactions between copper-containing species.

In a similar fashion, when copper oxides are in contact with carbon substrates, as might be the case if the copper oxides of azurite and malachite are used as pigments on a substrate containing charcoal, the Cu_2p core level might be lowered in terms of binding energy due to electron donation from the substrate, yielding characteristic spectroscopic signatures of these interfacial interactions [50]. The ability to distinguish these changes from the inherent differences in the core level binding energies of the different minerals, such as the 0.5eV difference between the two copper oxides of azurite and malachite, as measured by Kloprogge and Wood [40], critically depends on the availability of reference values and the expected range of these interfacial effects.

Lifetime Broadening and Shake-Up Satellites as Structural Indicators

Apart from the position of the main Cu $2p_{3/2}$ peak, the shape of the satellite structures and the extent of the "shake-up" satellites contain valuable additional information on the electronic structure of copper. For Cu (II) compounds, the "shake-up" satellites are due to the interaction of the photo hole created during photoemission of an electron from the Cu 2p orbital with the 3d electrons. This interaction leads to the creation of multiples that are observed as satellite peaks. The position of the satellite peaks depends on the configuration of the d electrons and the crystal field splitting of the 3d states. The latter depends on the coordination geometry and bond lengths. The Cu 2p XPS spectrum of azurite and malachite, given in the handbook compiled by [40], shows that for azurite, there are two satellite peaks at 940.3eV and 943.6eV. In contrast, for malachite, there are three satellite peaks at 938.9eV, 941.7eV, and 943.9eV. The presence of an additional satellite peak for malachite and the differences in the spacing of the satellite peaks for azurite and malachite are due to the differences in the crystal field environment of the Cu^{2+} ion in the two minerals. For azurite and malachite, where Cu (II) has a fixed position on the crystal lattice, the Cu 2p satellite structure is reproducible and unique. Changes in the satellite structure during storage may indicate changes in the coordination environment of the Cu^{2+} ion, e.g., loss of water or replacement of carbonate by oxide during dihydroxylation.

Additionally, effects of lifetime broadening, which are manifest through the total width and smoothness of the Cu 2p feature, have the potential to offer insight into the homogeneity and structural organization of the phase. Degraded pigments with some degree of amorphization will have Cu 2p features that are more broadened and diffuse in comparison to those of well-crystallized minerals like those found in the handbook. This is due to differences in photo hole lifetimes between ordered and disordered materials. This is particularly significant in differentiating between primary and secondary materials.

Practical Considerations for Quantification and Interpretation

In the context of quantitative XPS analysis of azurite, malachite, and their decomposition products, there are some best practices that are indicated by the literature and handbook data [40,46,49]: The choice of binding energy scale is of primary importance. The use of an adventitious carbon reference at 284.8eV for the carbon 1s peak, which is standard for XPS analysis, is a possible source of error if the carbon overlayer thickness or composition is different for different samples. Other authors have also chosen to use the Fermi level of the substrate or reference materials, each of which has its own implications for the binding energies obtained. The choice of a common reference scale for the analysis of azurite and malachite samples in the handbook allows for the direct comparison of binding energies for the two samples. The difference of 0.5eV is real and is not an artifact of calibration procedures.

Second, the Cu 2p photopeak's must be recorded at high energy resolution, i.e., analyzer pass energy ≤20eV for survey scans and ≤10eV for more detailed analysis. This is because lower resolution may not be sufficient for the resolution of closely spaced peaks such as Cu(I) and Cu (II) or for satellite peaks. The presence of high-resolution Cu 2p photopeak's for azurite and

How to cite this article: J Theo Kloprogge. The Use of X-Ray Photoelectron Spectroscopy in Studying Azurite and Malachite as Minerals, Pigments and in Secondary Products on Copper Objects. JOJ Material Sci. 2026; 10(3): 555788. DOI: 10.19080/JOJMS.2026.10.555788

malachite samples in the handbook indicates the level of detail that is possible for XPS analysis.

Third, the quantification should utilize sensitivity factors that are specific to the instruments and elements in question. The handbook provides both calculated and measured values for atomic percentages. This demonstrates the effect of the sensitivity factors used in the analysis.

Fourth, in the analysis of aged pigments and corroded surfaces, depth profiling using argon ion sputtering should be done with caution. This is because the different elements in the sample may be sputtered at different rates. In addition, Cu (II) may be reduced to Cu(I) and finally to metallic Cu. This effect may be compounded by the photo-induced reduction effect reported by [40] for malachite. It should be noted that the effect of the ion sputtering should be controlled.

Fifth, the analysis should be carried out with attention to the X-ray photon flux and the dwell time per spot. This is demonstrated in the handbook's documentation of the photo-induced Cu^{2+} to Cu^{+} reduction effect. This effect may be minimized by carrying out the analysis at a lower X-ray power or by reducing the dwell time per spot.

Lastly, the analysis should be complemented by other analytical methods such as X-ray diffraction to confirm the crystalline nature of the compounds. Raman spectroscopy may be used to identify the vibrational modes of specific compounds. In addition, transmission electron microscopy may be used to determine the distribution of the compounds at the nanometer scale. This is exemplified in the handbook's provision of both the XPS data and the composition of the sample.

Moreover, there are overlapping contributions from carbonate oxygen, hydroxyl groups, and chemisorbed species like water and/or other oxidizing species [33]. This is clearly demonstrated by the reference handbook values, where carbonate species are reported at 531.4eV and 531.3eV for azurite and malachite, respectively, compared to hydroxyl groups at 532.1eV and 532.0eV, respectively [50]. XPS analysis is based on homogeneous concentration profiles in the sampling depth. However, this is not true for azurite and malachite samples, particularly those with nonhomogeneous composition and/or surface alteration. The calculated atomic percentage values and Cu/O/C ratios based on XPS peak areas will not agree with the stoichiometric values. This is particularly true when surface effects are present, and this has been reported in aged pigments where leaching of certain species is known to affect the composition. The reference handbook values indicate large differences between calculated and measured atomic percentage values, particularly in malachite, where Cu was found to be 1.2% compared to a calculated value of 25.0%.

Integration with Complementary Techniques

With these limitations in mind, best practice for the characterization of azurite, malachite, and copper corrosion products involves the employment of multiple techniques, including XPS and X-ray diffraction (XRD), Fourier transform infrared spectroscopy (FTIR), Raman spectroscopy, and scanning electron microscopy (SEM). XRD offers the opportunity to identify the crystalline phase of the material, which can be correlated with the binding energies and peak shapes obtained by XPS. FTIR and Raman spectroscopy can confirm the presence of carbonate, hydroxide, and sulfate groups that often appear in the XPS spectrum and can overlap with the oxygen signal (Bertrand et al. 2013). SEM offers the opportunity to identify the morphology of the material, which can explain discrepancies in the XPS results due to differences in surface area effects and/or heterogeneous surface topography. For example, the degradation of the azurite and malachite pigments used in historical murals has been studied by employing multiple techniques to confirm that, indeed, azurite can degrade to the black oxide tenorite (CuO), which has the effect of changing the oxidation state of copper from a mixture of Cu(I) and Cu (II) to pure Cu (II), with corresponding changes in the XPS spectrum [51]. Without the aid of XRD to confirm the presence of the tenorite phase, the XPS results could have been misinterpreted.

Comparison of Pigment and Mineral XPS: Implications for Conservation and Archaeological Study

The ability of XPS spectroscopy to distinguish between primary azurite/malachite minerals and artificially synthesized or historically used pigments has been a challenge. Some of the synthesized pigments are characterized by unique impurities and crystal structure, but it has been established that XPS spectroscopy is unable to distinguish between the two, since the Cu (II) present in the mineral and the synthesized pigment has a similar coordination environment. The major breakthrough in the identification of the source of the pigment has been through trace element analysis and compositional data, indicating the limitations of XPS spectroscopy, which only provides partial information. In the context of conservation, the ability of XPS spectroscopy to detect secondary corrosion products, such as basic copper carbonates, chlorides, and sulfates, which form during storage of historical objects, has been significant, since these can be targeted for conservation treatment.

Conclusion

XPS has thus emerged as an invaluable tool for the characterization of the surface chemical makeup of the azurite and

How to cite this article:J Theo Kloprogge. The Use of X-Ray Photoelectron Spectroscopy in Studying Azurite and Malachite as Minerals, Pigments and in Secondary Products on Copper Objects. JOJ Material Sci. 2026; 10(3): 555788. DOI: 10.19080/JOJMS.2026.10.555788

malachite ore mineral, pigment, and copper corrosion product systems. However, in the interpretation of the XPS data for these systems, a number of possible artifacts must be taken into account. The comparative study of the ore mineral, the pigment, and the corrosion product systems highlights the major differences in the degree of surface homogeneity and the oxidation state distribution. It is apparent that the XPS technique is limited in the extent to which the differences in the chemical makeup of the three systems can be resolved. In addition to the lack of a set of standardized procedures for the measurement and data analysis for the three systems in the available scientific literature, the technique's inherent limitations imply that the quantitative XPS data for the three systems should be regarded as semi-quantitative in nature.

In the study of the chemical makeup of the patina layer in architectural copper and copper art objects, the XPS technique has shed light on the intricacy of the formation of the green corrosion layer. It is apparent from the study by [37] that the green corrosion layer observed in old copper roofs is a mixed phase compound whose chemical makeup is a reflection of the local environment. The study highlights the need for a proper understanding of the long-term durability of the copper. The observation of the formation of secondary copper compounds such as atacamite green and black tenorite in the degradation of the malachite and azurite pigments underscores the need to understand the chemical makeup of the degradation products in addition to the chemical makeup of the original pigment. The XPS technique is essential in the study of the chemical makeup of the degradation compounds in the malachite and azurite pigments.

References

1. Jabbour M, Ilmen S, Ikenne M, Zoheir B, Souhassou M, et al. (2025) Genesis of the At Abdellah copper deposit, Bou Azzer-El Graara inlier, Anti-Atlas, Morocco. Minerals 15(5): 545.
2. Effah (2025) Gold (Au) as a by-product of porphyry copper deposit mining. World Journal of Advanced Research and Reviews 28(02): 1559-1566.
3. Braxton DP, Cooke DR, Ignacio AM, Rye RO, Waters P (2009) Ultra-deep oxidation and exotic copper formation at the late Pliocene Boyongan and Bayugo porphyry copper-gold deposits: mineralogy, paleo altimetry, and their implications for geologic, physiographic, and tectonic controls. Economic Geology 104(3): 333-350.
4. Jadehkenary KA, Maghfouri S, Rastad E, Foltyn K (2025) Mineralization and geochemistry of sediment-hosted strata-bound copper (SSC) horizons in the Garedu Red Bed Formation of the Khormo-Gazak mining district, Tabas Block, Iran. Journal of the Geological Society 182(6): 2024-2071.
5. Bublikova TM, Setkova TV, Balitsky VS (2025) Thermodynamic modeling of phase formation conditions in the CuO-CO_2-H_2O-NH_3 system. Russian Journal of Inorganic Chemistry 70: 78-87.
6. Littva J, Bella P, Gál U, Herich P (2025) Geological setting and origin of Blue Cave with blue and green carbonate speleothems (Central Slovakia). Mineralia Slovaca 57(1): 5-38.
7. Xue ZF, Cheng W, Wang L, Xie Y (2022) Catalyzing urea hydrolysis using two-step microbial-induced carbonate precipitation for copper immobilization: perspective of pH regulation. Front Microbiol 13: 1001464.
8. Bloise A, Dattola L, Luca R, Miriello D (2023) Anglesite, cerussite, gypsum, langite, malachite, and posnjakite: new occurrences in the Calabria region (Southern Italy). Applied Sciences 13(4): 2200.
9. Frost RL, Martens W, Williams PA, Kloprogge JT (2002) Vibrational spectroscopy of azurite and malachite. Mineralogical Magazine 66(6): 1063-1073.
10. Frost RL, Martens WN, Rintoul L, Mahmutagic E, Kloprogge JT (2002) Raman spectroscopic study of azurite and malachite at 298 and 77 K. Journal of Raman Spectroscopy 33(4): 252-259.
11. Kloprogge JT, Frost RL, Hickey L (2004) FTIR and Raman study of malachite and azurite. American Mineralogist 89: 135-143.
12. Wu S, He M, Yang M, Peng B, Shi Y, et al. (2024) Near-infrared spectroscopic study of secondary minerals in the oxidation zones of copper-bearing deposits. Crystals 14(9): 791.
13. Shumilova MA, Pastukhova NN, Lomova NV, Kazantseva IS, Isupov NY, et al. (2025) Thermal decomposition of copper (II) hydroxide and hydroxycarbonates according to X-ray photoelectron spectroscopy in operando. Journal of Crystallography Crystalline Materials 240(5-6): 181-189.
14. Roy A (1993) Artists' pigments: a handbook of their history and characteristics. National Gallery of Art, Washington, DC, and Oxford University Press, Oxford, UK 2: 132.
15. Gravis D, Roy N, Ronzani NR, Houssiau L, Felten A, et al. (2023) Secondary ion mass spectrometry, a powerful tool for revealing ink formulations and animal skins in medieval manuscripts. Royal Society Open Science 10(6): 230059.
16. Zhu Y, Qi G, Guo Y, Wang D (2024) Analysis of decorative paintings in the Dragon and Tiger Hall of Yuzhen Palace: culture, materials, and technology. Coatings 14(8): 1022.
17. Amanatiadis S, Apostolidis G, Karagiannis G (2021) Consistent characterization of color degradation due to artificial aging procedures at popular pigments of Byzantine iconography. Minerals 11(7): 782.
18. Li Y, Hou X, Zhang X, Wang L, Li J, et al. (2023) Analytical characterization of wooden figurines excavated from the Tomb of Princess Yongtai, Qianling Tomb, China. Analytical Letters 57(2): 163-175.
19. Petiti C, Toniolo L, Berti L, Goidanich S (2023) Artistic and laboratory patinas on copper and bronze surfaces. Applied Sciences 13(21): 11873.
20. Dogra R, Puri M, Jamwal HS, Thakur SS (2026) Chemical analysis of historical materials and cultural heritage objects. International Journal of Research and Innovation in Applied Science (IJRIAS) 10(12): 743-753.
21. Čejka J, Sejkora J, Jebavá I, Xi Y, Couperthwaite SJ, et al. (2002) Raman spectroscopy of basic copper carbonates. Spectrochimica Acta Part A: Molecular and Biomolecular Spectroscopy 108: 171-176
22. Desmond DJ, Antonio JSP (2025) Fourier transform infrared (FTIR) database of historical pigments: a comparison between ATR-FTIR and DRIFT modalities. Applied Sciences 15(7): 3941.
23. Cortea IM, Ghervase L, Rădvan R, Serian G (2022) Assessment of easily accessible spectroscopic techniques coupled with multivariate analysis for the qualitative characterization and differentiation of earth pigments of various provenance. Minerals 12(6): 755.
24. Wang J, Yu Q, Yang Y (2024) Effects of UV light on traditional Chinese pigments: a study of malachite and azurite in silk paintings. Proceedings of SPIE 13418, Optics for Arts, Architecture, and Archaeology 9:

How to cite this article: J Theo Kloprogge. The Use of X-Ray Photoelectron Spectroscopy in Studying Azurite and Malachite as Minerals, Pigments and in Secondary Products on Copper Objects. JOJ Material Sci. 2026; 10(3): 555788. DOI: 10.19080/JOJMS.2026.10.555788

134183S.

25. Guglielmi V, Andreoli M, Comite V, Baroni A, Fermo P (2021) The combined use of SEM-EDX, Raman, ATR-FTIR and visible reflectance techniques for the characterization of Roman wall painting pigments from the Monte d'Oro area (Rome): an insight into red, yellow and pink shades. Environ Sci Pollut Res Int 29(20): 29419-29437.

26. Alves JF, Peixoto LPF, Oliveira LFCD (2025) Resonance Raman effect in copper carbonate minerals azurite and malachite. Journal of Raman Spectroscopy 56(11):1154-1161.

27. Lauwers D, Cattersel V, Vandamme L, Eester A, Langhe K, et al. (2014) Pigment identification of an illuminated mediaeval manuscript De Civitate Dei by means of a portable Raman equipment. Journal of Raman Spectroscopy 45(7): 1266-1271.

28. Eremin K, Stenger J, Green ML (2006) Raman spectroscopy of Japanese artists' materials: the Tale of Genji by Tosa Mitsunobu. Journal of Raman Spectroscopy 37(11): 1119-1124.

29. Botteon A, Lux A, Realini M, Strobbia P, Matousek P, et al. (2024) Raman spectroscopy advancements in heritage science. Proceedings of the EOS Annual Meeting (EOSAM 2024) 309: 14002.

30. Yogurtcu B, Cebi N, Koer A, Erarslan A (2024) A review of non-destructive Raman spectroscopy and chemometric techniques in the analysis of cultural heritage. Molecules 29(22): 5324.

31. Briggs D, Grant JT (2003) Surface analysis by Auger and X-ray photoelectron spectroscopy. IM Publications and Surface Spectra Limited, Chichester, UK, pp. 1-900.

32. Hu B, Huang L, Yang B, Xie X, Tong X, et al. (2022) Flotation performance and adsorption mechanism of a novel chelating collector for azurite. Minerals 12(4): 441.

33. Gao Z, Liu C, Lu T, Zhao Z, Wu G, et al. (2024) Understanding the adsorption mechanism of BTPA, DEPA, and DPPA in the separation of malachite from calcite and quartz: DFT and experimental studies. Minerals 14(7): 692.

34. Hradil D, Ermkov Z, Hradilová J, Bezdika P, Měková J (2024) Trace and minor element analysis of azurite blues in fine arts: possibilities and limitations in provenance studies. Appl Spectrosc 78(9): 1051-1062.

35. Watanabe M, Takaya M, Matsumoto M, Sakai J (2016) A comparative study of copper corrosion products formed at two hot spring sites. Corrosion Engineering 58(3): 143-151.

36. Watanabe M, Tomita M, Ichino T (2001) Characterization of corrosion products formed on copper in urban, rural/coastal, and hot spring areas. Journal of the Electrochemical Society 148(12): 522-528.

37. Bure R, Klajmon M, Fojt J, Rak P, Jílková K, et al. (2019) Artificial patination of copper and copper alloys in wet atmosphere with increased content of SO_2. Coatings 9(12): 837.

38. Biesinger MC, Lau LWM, Gerson AR, Smart R (2010) Resolving surface chemical states in XPS analysis of first-row transition metals, oxides and hydroxides: Sc, Ti, V, Cu and Zn. Applied Surface Science 257(3): 887-898.

39. Fu YC, Chen YC, Wu CM, Hsiao VKS (2023) Tailored nanoscale architectures for white light photo electrochemistry: zinc oxide nanorod-based copper oxide heterostructures. Coatings 13(12): 2403.

40. Kloprogge JT, Wood B (2020) Handbook of mineral spectroscopy. Volume 1: X-ray electron spectra. Amsterdam, Netherlands. Elsevier.

41. Giap AOH, Gong J, Hu X, Yue C, Feng Y (2024) MSL1 failure mechanism and solution for silicon carbide (SiC) power package with pressure-less sintering die-attach process on bare copper lead frame. Proceedings of the 2024 IEEE 26th Electronics Packaging Technology Conference (EPTC), pp. 740-745.

42. Park J, Son YG, Son CS, Hwang D (2024) Influence of oxygen flow rate on the phase structures and properties of copper oxide thin films deposited by RF magnetron sputtering. Coatings 14(8): 930.

43. Ligt B, Rollier FA, Wissink T, Chen W, Simons JFM, et al. (2024) Insights into the structure and activity of bimetallic Au/Cu_2O catalysts during CO_2 electroreduction to C_2 products. Journal of the Electrochemical Society MA2024-01.

44. Kunze S, Tănase LC, Prieto MJ, Grosse P, Scholten F, et al. (2021) Plasma-assisted oxidation of Cu (100) and Cu (111). Chemical Science 12: 14999-15009.

45. Matam SK, Sharma PK, Yu EH, Drivas C, Wilding M, et al. (2024) Electrochemical CO_2 reduction over Cu-based gas diffusion electrodes: a complementary spectroscopic study. Journal of the Electrochemical Society MA2024.

46. Franceschini F, Fernandes C, Schouteden K, Ustarroz J, Locquet JP, et al. (2025) Tailoring the glucose oxidation activity of anodized copper thin films. Catalysis Science & Technology 15(10): 3022-3035.

47. Lee HJ, Lee G, Lee HW, Lee TH, Kim IR, et al. (2024) Effects of post-deposition annealing on the electrical properties of Cu_2O/4H-SiC PiN diodes. Physica Status Solidi 221(23): 2400018.

48. Blaseio S, Dosche C, Rahaman M, Kiran K, Dworzak A, et al. (2024) Impact of Cu^+ and Cu^{2+} species on the oxide-metal transition processes of Cu_xO foams during the CO_2RR probed by operando quick-XAS. Journal of Materials Chemistry A 12(41): 28177-28192.

49. Sivkov DV, Petrova OV, Nekipelov SV, Vinogradov AS, Skandakov RN, et al. (2021) Identification of the Cu-O-C bond in Cu/MWCNTs hybrid nanocomposite by XPS and NEXAFS spectroscopy. Nanomaterials (Basel) 11(11): 2993.

50. Kriznar A, Kavkler K, Dolenec S (2024) Why are the early Gothic murals in St. Jacob's Church in Ormož, Slovenia, almost entirely black? Spectroscopy Journal 2(2): 37-52.

51. Schweitzer LC, Mathew A (2001) Corrosion products on archaeological copper alloys. Journal of the American Institute for Conservation 40: 1-13.

How to cite this article: J Theo Kloprogge. The Use of X-Ray Photoelectron Spectroscopy in Studying Azurite and Malachite as Minerals, Pigments and in Secondary Products on Copper Objects. JOJ Material Sci. 2026; 10(3): 555788. DOI: 10.19080/JOJMS.2026.10.555788

DOI: 10.19080/JOJMS.2026.10.555788

How to cite this article: J Theo Kloprogge. The Use of X-Ray Photoelectron Spectroscopy in Studying Azurite and Malachite as Minerals, Pigments and in Secondary Products on Copper Objects. JOJ Material Sci. 2026; 10(3): 555788. DOI: 10.19080/JOJMS.2026.10.555788